Saturation Effect in Microwave Absorption of Ammonia*

ROBERT L. CARTER AND WILLIAM V. SMITH
Department of Physics, Duke University, Durham, North Carolina

(Received January 12, 1948)

Attenuation and line width for the NH_3 3,3 line are measured as a function of the intensity of radiation incident on the gas for several different pressures. The saturation effects are found to be proportional to the power and inversely proportional to the square of the line width, in agreement with theory. An estimate of the collision cross section given by saturation data is in agreement with that deduced from collision broadening data.

I. INTRODUCTION

THE use of vacuum tube oscillators as high intensity monochromatic sources for certain types of spectra has initiated investigations of "saturation" phenomena in which absorption or induced emission varies with intensity of the incident radiation, since the latter can be made sufficiently intense to disturb the thermal equilibrium of the irradiated material. While the earliest experiments of this sort are in the field of nuclear induction in the solid state,[1] recent experiments by Townes[2] have shown that similar effects exist in molecular absorption in the microwave region. The only molecule quantitatively studied so far is ammonia, and, more specifically, the 3,3 member of the inversion spectrum at 23,870 megacycles, as this line, with an absorption for plane waves of about 8×10^{-4} cm^{-1} is the strongest yet discovered in the microwave region.[2,3] In spite of this high absorption, experimental results of different investigators are in marked disagreement as to the amount of broadening accompanying saturation.[2,4-6] In our own investigations we find that an underestimation of certain systematic errors masked a broadening which we now find to be observable, but still somewhat less than quoted by Townes. Our present observations taken before the publication of Pond and Cannon's letter[6] agree with their data, and extend the data to higher pressures. A quantitative agreement with theory is now found.**

II. THEORY

Of the several possible mechanisms proposed by Townes, which might lead to saturation, the only one now believed to be operative is the disturbance of the distribution of molecules between the ground and excited states.[7] This arises when the rate of absorption of energy per molecule in the ground state becomes comparable with the collision rate between molecules. The resulting modification of Van Vleck and Weisskopf's relation[8] for the absorption of pressure broadened lines under conditions where the line width is small compared to the frequency can be shown to be

$$\gamma(\nu)=\frac{\gamma_0}{\left(\frac{\nu-\nu_0}{\Delta\nu_0}\right)^2+1+\frac{AP}{(\Delta\nu_0)^2}} \tag{1}$$

with the line width at half-power

$$2\Delta\nu=2\Delta\nu_0\left(1+\frac{AP}{(\Delta\nu_0)^2}\right)^{\frac{1}{2}}, \tag{2}$$

where

γ_0 = peak unsaturated attenuation = attenuation at resonant frequency, ν_0, for low input power

$$=\frac{8\pi^2\nu^2n_0}{3ckT\Delta\nu_0}|\mu_{jk}|^2 \text{ in cm}^{-1},$$

* The research described in this report was supported by Contract No. W-28-099-ac125 with the Army Air Forces, Watson Laboratories, Air Materiel Command.

[1] F. Bloch, Phys. Rev. **70**, 460 (1946); F. Bloch, W. W. Hansen, and M. Packard, Phys. Rev. **70**, 474 (1946); Purcell, Torrey, and Pound, Phys. Rev. **69**, 37 (1946).

[2] H. Townes, Phys. Rev. **70**, 665 (1946).

[3] B. Bleaney and R. P. Penrose, Proc. Roy. Soc. **189**, 358 (1947).

[4] W. Gordy and M. Kessler, Phys. Rev. **71**, 640 (1947).

[5] W. V. Smith and R. L. Carter, Phys. Rev. **72**, 638 (1947).

[6] T. A. Pond and W. F. Cannon, Phys. Rev. **72**, 1121 (1947).

** Subsequent to submission of this manuscript a very thorough paper on saturation in ammonia by Bleaney and Penrose, Proc. Phys. Soc. **60**, 83 (1948), has appeared. Their results are in substantial agreement with ours.

[7] J. Schwinger and R. Karplus, private communication.

[8] J. H. Van Vleck and V. F. Weisskopf, Rev. Mod. Phys. **17**, 227 (1945).

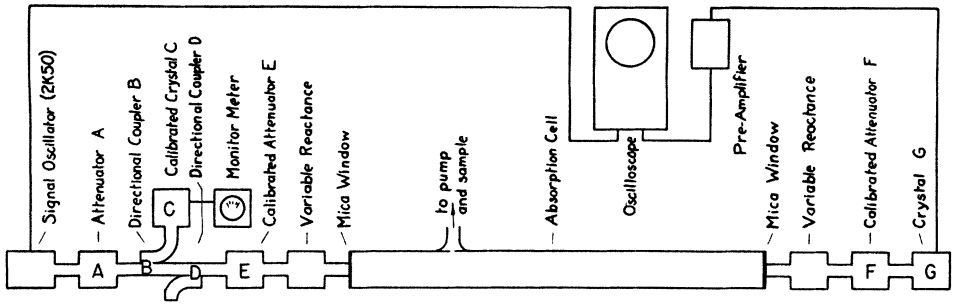

FIG. 1. Block diagram of apparatus.

$2\Delta\nu_0$ = half-power line width at low input power,
n_0 = number of molecules in the 3,3 ground state for thermal equilibrium,
P = input power in ergs/cm² sec.,

$$|\mu_{ij}|^2=\frac{K^2}{J(J+1)}\mu^2 \text{ where } K=J=3,$$

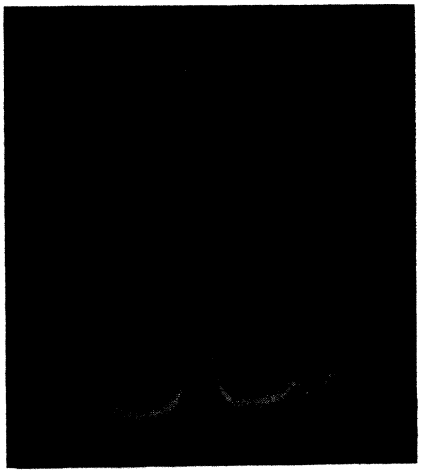

(a)

(b)

FIG. 2. Ammonia 3,3 line with input to crystal 0.15×10^{-6} watt $2\Delta\nu_0 \leqq 300$ kc. (a) Input to cell $=1.5\times10^{-6}$ watt; (b) input to cell $=150\times10^{-6}$ watt.

μ = dipole moment $=1.45\times10^{-18}$ e.s.u.,

$$A=\frac{8\pi|\mu_{ij}|^2}{3ch^2}=1.02\times10^7,^{***}$$

h, c, k, T = Planck's constant, velocity of light, Boltzmann constant, and absolute temperature, respectively.

Expressions (1) and (2) assume a non-degenerate line with pressure broadening and saturation the sole causes for line width. Constant power along the guide and over the cross section is also assumed. The first condition is approximately attained experimentally, but not the second.

Averaging over the guide cross section and replacing the unsaturated absorption at ν_0 by $(\lambda_g\gamma_0/\lambda)$ replaces Eqs. (1) and (2) by

$$\langle\gamma(\nu)\rangle_{Av}=\frac{\gamma_0}{\alpha}\left\{1-1\Big/\left(1+\frac{2\alpha}{((\nu-\nu_0)/\Delta\nu_0)^2+1}\right)^{\frac{1}{2}}\right\}\frac{\lambda g}{\lambda}, \quad (3)$$

and

$$\langle 2\Delta\nu\rangle_{Av}=2\Delta\nu_0\left(\frac{2\alpha^2-\alpha-1+(1+2\alpha)^{\frac{1}{2}}(1+2\alpha)}{1+3\alpha-(1+2\alpha)^{\frac{1}{2}}}\right)^{\frac{1}{2}}, \quad (4)$$

where $\alpha=[A\bar{P}/(\Delta\nu_0)^2](\lambda g/\lambda)$ and $\bar{P}$ is the average power density over the guide cross sections.

Despite the complicated forms of Eqs. (3) and (4), they differ only to a minor extent from the unaveraged expressions, as is evident from

*** This value neglects averaging over the Zeeman components of the line. Proper averaging yields more complicated expressions than those used here,[7] and, to a first approximation, gives a value of $A=1.75\times10^7$.

(a) (b)

FIG. 3. Ammonia 3,3 line with gain adjusted for approximately constant height; $2\Delta\nu_0 \cong 300$ kc. (a) Input to cell $= 1.5 \times 10^{-6}$ watt; (b) input to cell $= 150 \times 10^{-6}$ watt.

Figs. 4 and 5. If the average power density is used in Eqs. (1) and (2), the ratio of (1) to (3) is unity at both low and high powers, while the ratio of (2) to (4) is unity at low powers and $(\frac{3}{2})^{\frac{1}{2}}$ at high powers. This small variation is reasonable, since in the average the low power regions of the guide cross section contribute little to the power absorbed per unit length. It should be noted that variation in power over the guide length is a more serious factor, as it is the relative power absorbed per unit length that counts in the total observed attenuation. Indeed, this power variation along the guide length probably accounts for one of the failures to observe saturation.[4] The cell length of 2 meters used in the present work is short enough to avoid this difficulty, as its attenuation in the absence of ammonia is only 1 decibel.

III. EXPERIMENTAL METHOD

The apparatus used is shown schematically in Fig. 1. The signal oscillator was a Western Electric 2K50 reflex klystron. A saw-tooth voltage derived from a DuMont oscilloscope was applied to the reflector of the tube. The voltage used was sufficient to sweep the tube about 10 megacycles, over which range the variation in output power was very small, as the 2K50 reflector modes are about 100 megacycles wide. Attenuator A was adjusted to maintain a constant reading on crystal C, which was calibrated against a thermistor. The small reflections set up by the mica windows of the cell were balanced out by variable reactances. The quality of match was checked both by minimizing reflections observed at directional coupler D, and by obtaining a smooth mode presentation on the scope which was connected to a crystal G through a preamplifier. The crystal also was tuned to eliminate reflections. In general, calibrated attenuators E and F were varied together to vary power input to the cell while maintaining the input to crystal G at a constant level in the region where the crystal response was proportional to power, thus eliminating any possibility that variation in line shape might result from crystal saturation. An additional result of the use of constant crystal input was a constant noise level and constant (small) curvature of the base line.

The preamplifier and oscilloscope have a flat response from 10 to 100,000 cycles. As a sweep frequency of 120 cycles was used, in general, no distortion was present in reproducing absorption lines covering from 1 percent to 10 percent of the sweep length. Variation in sweep speed checked the flatness of the response.

We have made no direct pressure measurements, preferring to present our data as a function of the unsaturated line width $2\Delta\nu_0$, which was accurately measured by photographing both the main line and the fine structure, the latter establishing the frequency scale.[9]

Both the 2K50 and the preamplifier were battery operated to minimize hum and fluctua-

tions. The cell length of 2 meters gave an attenuation in the absence of ammonia of only one decibel, so that the power could be considered sensibly constant over the cell length. The cell cross section was 10.7×4.3 mm.

The data were obtained as 35-mm photographs of a five-inch oscilloscope screen; they were examined in enlarged projection. Typical pictures are shown in Figs. 2 and 3. The crystal input power was the same for Figs. 2a and 2b, while the power through the cell was 100 times as large for 2b as 2a. The factor of difference in peak attenuation is clearly seen, while the factor of differences in line width can only be measured by enlargement from the original film. In Figs. 3a and 3b, attenuator F is maintained constant while the oscilloscope gain is varied to maintain constant line height. There is the same factor of 100 in input power to the cell, and here the change in line width is evident although changes in curvature in the background make the measurements uncertain by about 20 percent.

IV. EXPERIMENTAL RESULTS AND COMPARISON WITH THEORY

Figure 4 shows a plot of $\gamma(\nu_0)$ *versus* input power P to the cell for three different pressures. The vertical scale is arbitrary, the different curves being displaced relative to one another to facilitate comparison. Each curve approaches a constant asymptote at low input powers. (The asymptotes for the different curves differ by a few percent from the theoretically constant value.) For curve C, the highest pressure at which the fine structure could be clearly resolved, the asymptote is taken as 7.7×10^{-4} cm^{-1}, less by 10 percent than the value of 8.6×10^{-4} cm^{-1} which we measured independently at higher pressures with an 8-meter cell. The departure of absorbed power from linearity with γ, while

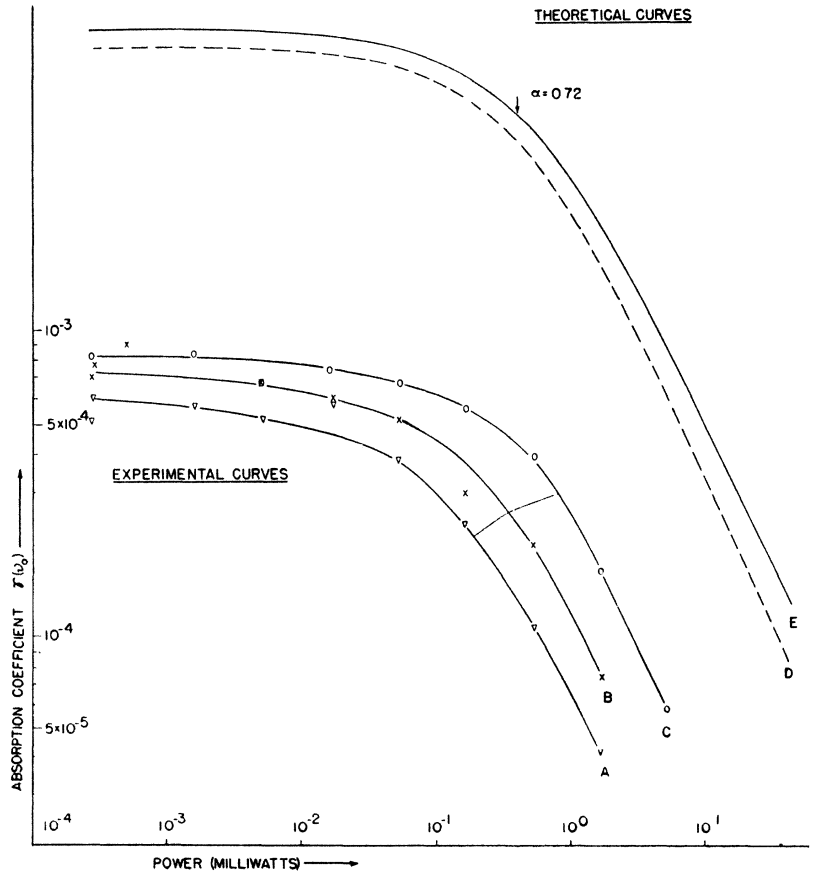

FIG. 4. Peak attenuation of $N^{14}H_3$ 3,3 line as function of power. Experimental curves (A, B, and C) taken at successively higher pressures. Theoretical curves were fitted to C at $\gamma/\gamma_0=0.5$ and displaced vertically. Curves D and E were obtained from unaveraged theory (Eq. (1)) and averaged theory (Eq. (3)), respectively.

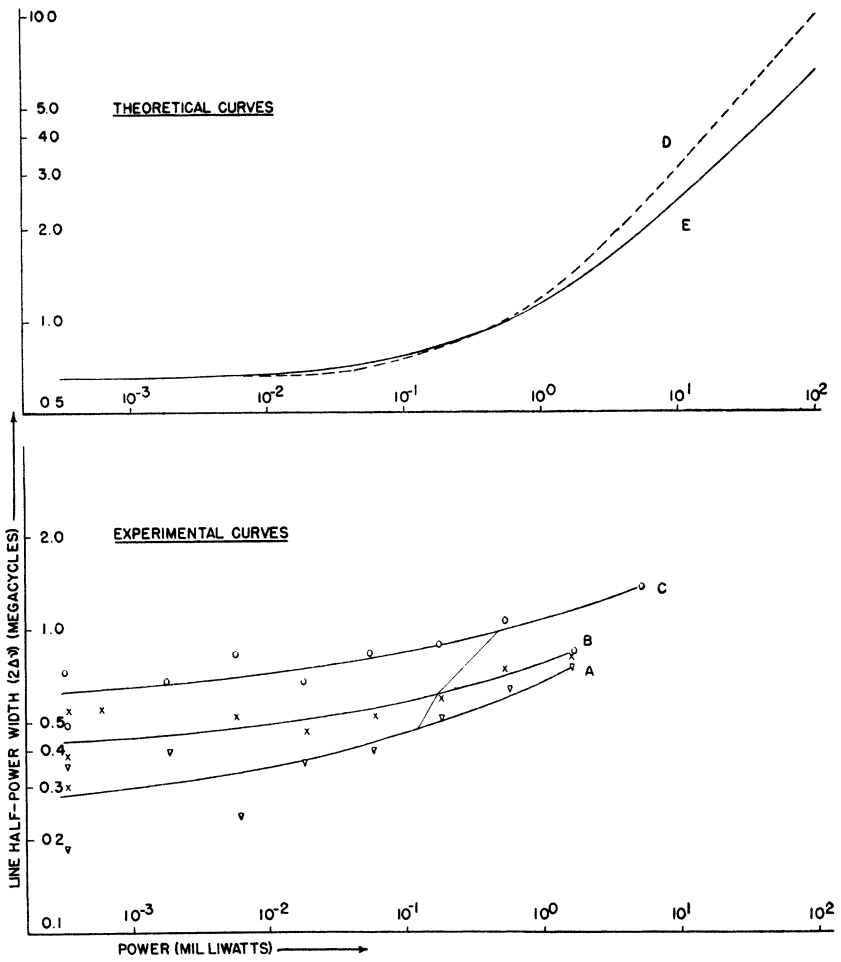

FIG. 5. Line width of the $N^{15}H_3$ 3,3 line as a function of power. Experimental curves A, B, and C correspond to curves A, B, and C of Fig. 4. Theoretical curves were fitted to C at $\gamma/\gamma_0=0.5$. Curves D and E were obtained from unaveraged theory (Eq. (2)) and averaged theory (Eq. (4)), respectively.

small for these values of γ, has been corrected for in the data. Also plotted on the graph are theoretical curves D and E, fitted to curve C at the observed half-power point, and displaced vertically to facilitate comparison.

It is clear that a combination of vertical and horizontal displacements of the curves A and B will superpose both on C within the 20 percent error estimated in our observations. To this accuracy, the data can also be fitted to either theoretical curve, although the averaged curve E will be taken as correct.

Since the theoretical curves are functions of the ratio $[P/(\Delta\nu_0)^2]$, it is clear that the horizontal displacements of $4db$ and $6db$ (2.5 and 4 in power ratios) necessary to superpose A and B on C should correspond to ratios of line width of 1.6 and 2, respectively. Examining Fig. 5, in which a similar comparison of experiment with theory is made for the line widths, the respective ratios are found to be 1.6 and 2.2. Since the line widths are estimated to be accurate to only 20 percent, the agreement with theory is more than satisfactory. That the observed scatter in the data at the low input power end of the graph is more than this 20 percent estimate is due to the fact that the data were taken with the system sealed off from the pumps, and ammonia absorbed on the walls was released during the run, which was taken from low to high powers and back to low in interlocking steps; an average of the data thus represents a run at constant pressure.

Finally, the constant A was calculated from the data of Fig. 4 and the corresponding half-power line width at low powers obtained from Fig. 5. The value of A is very sensitive to $\Delta\nu_0$,

and the 20 percent uncertainty in $\Delta\nu_0$ rendered the value of A thus obtained too inaccurate for satisfactory check. Additional data were taken in which the pressure variation during a run was reduced to a negligible amount, and values of $\Delta\nu_0$ showing variations of less than 10 percent were obtained. From these data a value of $A=(1.6\pm0.3)\times10^7$ cm^2/erg sec. was calculated, agreeing with the theoretical value when Zeeman averaging is included.

PHYSICAL REVIEW VOLUME 73, NUMBER 9 MAY 1, 1948

Secondary Electron Emission from Targets of Barium-Strontium Oxide

J. B. JOHNSON
Bell Telephone Laboratories, Incorporated, Murray Hill, New Jersey
(Received December 22, 1947)

The secondary electron yield of (BaSr)O has been studied, as induced by microsecond pulses of primary electrons with energy up to 2000 ev. The δ *vs.* V_p curves have the usual form, with maximum δ near 1200 ev. At room temperature, and before surface charges build up, the δ_{max} is of the order 12, but it may be reduced to 6 by less than 0.1 atomic layer of Ba evaporated from a nearby thermionic cathode. With increasing temperature δ decreases to an apparent minimum at ~600°C. With the onset of d.c. thermionic emission the total yield increases during each pulse, in rough proportion to the thermionic current. The increase is thought to represent a transient change in thermionic activity caused by the bombardment. No change with temperature is observed for the energy distribution of the true secondaries. The possibility of field-enhanced secondary emission at low temperatures is considered.

I. INTRODUCTION

IN earlier short notes and abstracts some results of pulsed measurements on the secondary emission properties of thermionic oxide cathodes were described.[1] Briefly, the results were these: The yield δ of secondary electrons from oxide cathodes is relatively high, from 4 to 10 at the optimum voltage, depending on various conditions. Near room temperature the δ tends to be high, decreasing slowly with temperature up to 600°C. In the temperature region where thermionic emission is appreciable, an increase in the thermionic emission occurs during and shortly after the bombardment with primary electrons and this emission is superimposed on the secondary current.

These measurements have now been amplified and extended and will be described more fully in this paper. The earlier conclusions are supported in all essentials, particularly as regards the presence of the bombardment-enhanced thermionic emission. The principal results of the measurements on secondary emission are given in Section 4.0 of the paper, which deals with the influence of the various parameters such as primary energy, temperature, current density, and other factors on the secondary emission ratio of the oxide target. The test circuit and the general characteristics of the experimental tubes are dealt with in Section 2.0. In Section 3.0 are described the specific characteristics of a particular tube and target from which the typical results in Section 4.0 were derived, involving the determination of temperature, thermionic activity, and the possible limitations imposed on the measurements by space charge in the tube. Matters which do not bear directly on the main results of Section 4.0 but which are still of considerable interest are dealt with in the last four sections. These include the effects of barium poisoning, the primary energy at which $\delta=1$, the energy of the secondary electrons, and the possible effects of high internal field in the target.

Two other reports on the secondary yield of oxide cathodes have appeared in recent years. The first, by Morgulis and Nagorsky,[2] presents

[1] J. B. Johnson, Phys. Rev. 66, 352 (1944); Phys. Rev. 69, 693 (1946); Phys. Rev. 69, 702 (1946).

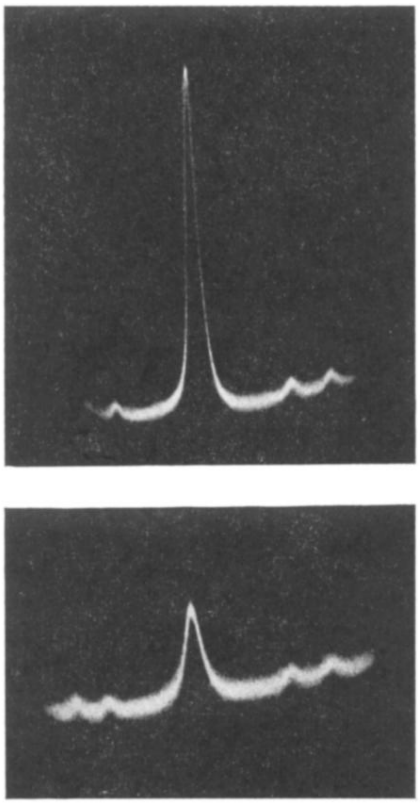

(a)

(b)

FIG. 2. Ammonia 3,3 line with input to crystal 0.15×10^{-6} watt $2\Delta\nu_0 \cong 300$ kc. (a) Input to cell $= 1.5\times10^{-6}$ watt; (b) input to cell $= 150\times10^{-6}$ watt.

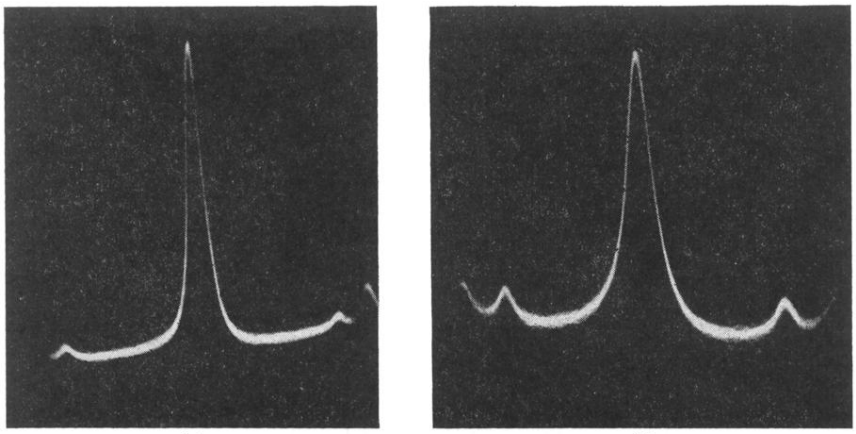

(a) (b)

FIG. 3. Ammonia 3,3 line with gain adjusted for approximately constant height; $2\Delta\nu_0 \cong 300$ kc. (a) Input to cell $= 1.5 \times 10^{-6}$ watt; (b) input to cell $= 150 \times 10^{-6}$ watt.